Co-Design of Cyanobacteria Mutant Strains and Processes for Phosphorus Recovery from Livestock Wastewater

Theodore A. Chavkin[1]†, Leonardo D. González[1]†, Brenda Cansino-Loeza[1], Rebecca Larson[2], Brian F. Pfleger[1*], Victor M. Zavala[1*]

1 Department of Chemical and Biological Engineering, University of Wisconsin-Madison, 1415 Engineering Drive, Madison, WI, USA, 53706
2 Department of Civil and Environmental Engineering, University of Wisconsin-Madison, 1415 Engineering Drive, Madison, WI, USA, 53706
†Contributed equally to this work
*Corresponding Authors: brian.pfleger@wisc.edu, zavalatejeda@wisc.edu

Abstract

Livestock agriculture generally operates as a linear economy, consuming large quantities of nonrenewable energy and nutrients while generating waste that often pollutes the environment. In this work, we propose approaches to help mitigate nutrient pollution via the development of cyanobacteria-based processes that capture phosphorus from dairy manure. Using engineered strains of cyanobacteria, we were able to increase biomass phosphorus density 8.5-fold with no impact on growth rate, producing biomass that contained 14% phosphorus by mass. Techno-economic modeling revealed that the dramatic increase in phosphorus density leads to a significantly more cost- and resource-efficient process, with over a 2-fold reduction in total annualized cost (TAC), 8-fold reduction in required land use, 3-fold reduction in energy usage, and fully eliminating the use of freshwater. Further analysis showed that combining the mutant strain with a simplified nutrient recovery process resulted in a phosphorus recovery charge (PRC) of 9.2 USD per kg P, which is 88% lower than an estimated socioeconomic cost of P runoff (75 USD per kg P) and equivalent to a service charge of 0.015 USD/gal of manure processed. By using cyanobacteria biomass as a P-dense biofertilizer, the proposed approach can help facilitate nutrient transportation and the transition to a more circular agricultural economy.

Keywords: Techno-economic analysis (TEA), Anaerobic digestion (AD), Dairy wastewater, Biofertilizer, Algal wastewater treatment, Synthetic biology, Photobioreactors (PBR)

Introduction

Phosphorus (P) is an essential element for life that, along with nitrogen (N) and potassium, forms the core of most synthetic fertilizers. The demand for increased agricultural yields driven by the need to feed a growing population has resulted in global phosphorus fertilizer application tripling over the last 60 years.[1] However, modern phosphorus fertilizer production is unsustainable. Approximately 80% of the phosphorus used for agricultural production is sourced from phosphate rock deposits which were formed over millions of years.[2] These deposits are a non-renewable resource, and the accelerated rate of depletion has raised concerns over a "peak phosphorus" event in the near future, where increased resource scarcity results in shortages and increased prices.[2,3] Such a scenario would undoubtedly affect vulnerable, low-income communities the most, putting them at an increased risk of food insecurity and malnutrition.

Phosphorus management is especially important in dairy farming, where large quantities of N- and P-rich dairy manure are generated and routinely used as fertilizer. The low N:P ratio of dairy manure does not match the nutrient requirements of most crops; this promotes the overapplication of manure and accumulation of P in soil.[4,5] The nutrient content of manure varies by farm and season, but generally has an N:P ratio of ~6:1.[6] When applied to fields to meet the nitrogen demand of corn (which requires an N:P ratio of 7:1), this leads to roughly 15% of the applied P being left unconsumed. Rain can mobilize excess soil P and deposit it in local waterways, representing a loss of valuable and non-renewable nutrients.[7] P runoff into waterways also supports harmful algal blooms in lakes and other waterbodies, a process known as eutrophication. In addition to the severe environmental damage they cause in aquatic ecosystems, harmful algal blooms also have significant health and economic costs on the residents living around eutrophic waterbodies.[8] For instance, it has been estimated that leaching one kg of phosphorus into waterways can lead to socioeconomic costs that reach 75 USD, due to the combined loss of recreational/tourism activities and to impacts on property values.[9]

Technologies that support more sustainable manure management practices have existed for decades. Anaerobic digestion (AD) systems process raw manure by feeding it to microorganisms that generate biogas, a mixture largely composed of CH_4 and CO_2. The primary benefit of AD treatment is the generation of methane as a renewable fuel that can be used for electricity generation, heating, or as a transportation fuel. The unconsumed material left over after AD treatment and solids separation (known as digestate) contains most of the nutrients from the raw manure and is typically applied as a liquid fertilizer. Critically, while AD reduces methane emissions from manure, it does not address the N:P imbalance. As a result, digestate application has the same potential for overapplication of P and eutrophication as manure application.[6]

One avenue for balancing nutrients in wastewater is biological nutrient recovery, typically using phosphate accumulating organisms (PAOs).[10,11] Cyanobacteria have gained particular interest in the biological nutrient recovery space,[12-14] as photosynthesis allows cyanobacteria cultivation to be a net consumer of CO_2 and operate in inexpensive fermenters like open raceway ponds or bag photobioreactors (b-PBRs).[15] In contrast to heterotrophic PAOs, autotrophic PAOs like cyanobacteria do not require a fixed carbon source, allowing them to be deployed in carbon-poor waste streams like anaerobic digestate without the need for an additional fermentable carbon source.[16,17] Previous work has demonstrated that cyanobacteria can be grown using nutrient-rich waste streams such as digested dairy manure.[18-20] The produced biomass can serve as an effective biofertilizer when combined with synthetic fertilizers resulting in similar crop yields, slower nutrient release (which reduces soil leaching), and a smaller carbon footprint when compared to using synthetic fertilizers alone.[21-23] Furthermore, the use of biofertilizer can also enrich soils by increasing organic carbon content, decreasing soil erosion risk, and improving the health and diversity of microbial and fungal communities.[24-26] Using modern genetic tools, cyanobacteria have been modified to produce fuels, feed additives, and commodity chemicals, enabling co-production of value-added chemicals in a waste management process.[15] While previous work has explored the development of cyanobacteria-driven nutrient recovery processes,[12-14,21-31] the use of genetic engineering to improve process performance is less studied.

In this work, we present a nutrient recovery process that combines anaerobic digestion and cyanobacteria cultivation. We used process modeling and techno-economic analysis for assessing how changing parameters of the cyanobacteria cultivation and strain design affect key economic metrics such as the cost of recovering the phosphorus in manure, capital and operating costs, and resource use (land,

water, and energy). We then use the insights from techno-economic analysis to engineer new strains of *Picosynechococcus* sp. PCC 7002 (referred to as "7002" hereafter) for use in phosphorus bioaccumulation. The proposed process generates a dense, nutrient-rich biomass that can be used as a biofertilizer, enabling long-distance transportation and potentially facilitating the transition to a more circular agricultural economy.

Experimental Section

Process Model Description

The baseline design for the process is illustrated in Figure 1. The front-end is comprised of an AD system that takes in raw manure and produces biogas along with digestate. The biogas is sent to a pair of scrubbers to remove any H_2S, a corrosive compound that can damage downstream units, and CO_2 present. The resulting product is a high-purity methane (CH_4) stream that is either exported or routed to a cogeneration unit where it is mixed with air and combusted to generate electricity and heat. The products of methane combustion, a flue gas composed of N_2, H_2O, and CO_2, are then mixed with the scrubbed CO_2 and routed to the b-PBRs where the CO_2 can be absorbed by the cyanobacteria via photosynthesis. The fraction of biogas exported off-site (sold to generate revenue) can be varied depending on market conditions, such as gas and electricity prices, capital costs of the power generation system, and the utility demands of the farm. In our baseline design, we set the export fraction to 71% of the biogas produced. This allows us to generate enough CO_2 to meet the carbon requirements of the cyanobacteria cultivation system.

The digestate that forms in the AD is sent to a solid-liquid separator (SLS) where larger solids are removed to be used as animal bedding. The SLS enables the recovery of approximately 30% of the P, or 3.8 tonnes/yr, which is removed in the solids stream. Meanwhile, the liquid stream is fed to a series of b-PBRs where it is used as a nutrient-rich medium to grow the cyanobacteria. In addition to the digestate, an additional nitrogen source (urea) can also be fed to the reactors (if necessary) to provide any additional N required to meet the nutrient needs of the cyanobacteria. Growth is assumed to be light-limited and is simulated as described by Clark et al.[32] After harvesting, the culture enters a flocculation system where self-flocculation is induced. The outlet of this unit is fed to a lamella clarifier where the flocs settle out of solution and are then sent to a pressure filter to produce a concentrated biomass solution. This solution is transferred to a thermal dryer that completes the moisture removal and yields a dry cyanobacteria biomass product. The biomass-free water exiting the lamella clarifier and pressure filter is mixed and 95% is recycled back to the b-PBRs while the remaining 5% is purged to prevent the buildup of impurities in the process. While the manure supplies water to the process, this is not sufficient in the baseline process to compensate for water losses in the purge and thermal dryer. As a result, an additional stream of freshwater must be fed into the b-PBRs.

Using a techno-economic model of the process, we calculated the total annual cost (TAC) of the biofertilizer production facility based on a 15% DROI and a 15-year process life. The revenues generated by the natural gas and electricity produced by the process are based on typical market prices. The price of the cyanobacteria biofertilizer is based on the cost of obtaining an equivalent amount of nutrients from diammonium phosphate (DAP), a commonly used synthetic fertilizer. Revenue can either be in the form of a direct payment for products that are exported off-site or in the savings associated with reductions in the amounts of utilities and fertilizer that are purchased from the market when the products are consumed on-site. The difference between the product revenues and the TAC is covered in the form of a phosphorus

recovery charge (PRC), which is interpreted as a service cost per kg of P captured by the process. We compared this service cost with the socioeconomic cost of P runoff reported in the literature. This provided context for the PRC and allowed us to gauge if the process was able to provide a net benefit to society. The PRC served as the primary performance metric in our analysis.

In addition to the PRC, we also measured the overall costs and resource needs/footprints of the process. In our study, we measured economic intensity using the total annual cost (TAC) of the process, which is calculated from the total capital investment (TCI) and the total operating cost (TOC). Resource intensity was measured by the energy, land, and freshwater required by the process. These metrics are obtained using the TEA process model (see Data Availability Statement below). All data and code needed for reproducing the results are shared with the manuscript.

Cyanobacteria mutant construction

Picosynechococcus sp. PCC 7002 growth was performed in Media AD7.[33] Liquid cultures were grown in a custom Kuhner shaking incubator at 37˚C, 250µE/m^2/s light intensity, and a constant 1% CO2 atmosphere. Plate cultures were grown on media A with 1.5g/L Bacto agar, and incubated at 37˚C, 200µE/m2/s light intensity, and a constant 1% CO2 atmosphere. Genes of interest were cloned from *Synechococcus elongatus* sp. 2973 into E. coli shuttle vectors along with a gentamycin resistance cassette and 750bp of homology to the 7002 genome up- and down-stream. Constructs were assembled using isothermal assembly, propagated in E. coli, then purified for transformation into 7002. 7002 was grown in media A+ to OD730 of 0.5-1.0, then centrifuged and resuspended in $1/10^{th}$ volume. To this concentrated stock, 0.5-1µg of DNA was added to 1mL of concentrated cells, then incubated for 3 hours at 37˚C with 200µE light intensity without shaking or CO_2 addition. After transformation, cells were plated on media A agar plates with 10µg/L gentamycin. After 1-3 days, colonies were pooled into liquid media A with 30µg/L gentamycin, grown overnight, and plated on media A agar plates with 30µg/L gentamycin. Individual colonies were screened via PCR to ensure they were homozygous and patched if needed onto subsequent media A plates with 30µg/L gentamycin.

Phosphorus uptake experiments

Cultures of 7002 were inoculated at an initial OD_{730} of 0.1 from stationary precultures in media A+ with indicated concentrations of phosphate as KH_2PO_4. Cultures were incubated in 25mL shake flasks as stated above in a custom Kuhner shaking incubator at 37˚C with 250µE light intensity and 1% constant CO2 atmosphere. For sampling, flask weight was recorded at the beginning of each experiment, then re-weighed at each time point. Sterile filtered water was added to account for evaporation by weight, and 1mL was removed at each time point, adjusting the flask weight by assuming 1mL = 1g. Samples were centrifuged at 6,000g for 1 minute and spent media removed. Pellets and spent media were stored at -20˚C until analysis.

Media phosphorus was quantified using Hach PhosVer reagent and Hach method 8048. Briefly, samples were diluted in sterile filtered water 50-fold to a final volume of 10mL, ensuring that all glassware was free of residual phosphate with an acid wash. To each sample one sachet of PhosVer 3 was added and mixed by inversion for 15 seconds. Samples were incubated for 2 minutes at room temperature, then measured via UV-Vis spectrophotometer for absorbance at 880nm. Samples were quantified using a 4 point

standard curve and discarded if outside the linear range. Samples were quantified within 8 minutes of reagent addition.

Photobioreactor cultivation

Photobioreactor (PBR) experiments were carried out in custom lab built 1L reactors.[34] Initial volume was set to 800mL of media A with 5mM phosphate and 10mM calcium. PBRs were illuminated and heated with adjustable daylight LEDs set to 750µE/m2/s light delivery at the surface of the reactor. Mixing was achieved with a magnetic stir bar set to 500rpm and reactors were sparged with 5% CO_2 balanced with air at 0.1LPM through a sintered sparging stone.

Seed cultures were inoculated from frozen stock in 25mL media A and grown to stationary phase, then subinoculated into 40mL media A at an OD730 of 1.0 to synchronize growth and grown overnight. PBRs were inoculated to an OD730 of 0.1 and induced after 24 hours with 1mM IPTG. At 24 hours, phosphate feeding was achieved with constant flow of 200mM K_2HPO_4 through a 3-channel peristaltic pump and feed rates were monitored by measuring reduction in mass over time.

Specific gravity and settling quantification

To quantify settling rate, samples were taken from 72 hour fed batch PBR cultures and diluted in sterile 0.9% NaCl to an OD730 of 0.8. 100µL was aliquoted into each well of a round bottom 96 well plate, with 100µL 0.9% NaCl as blank sample. Absorbance was measured at 730nm every 90 seconds for 30 minutes without shaking in a Tecan M1000 plate reader.

Specific gravity was measured as described previously for microalgae.[35] $CsCl_2$ was dissolved in water to a concentration of 100% w/v, then diluted to 90%, 80%, and 70%. Blue dye was added to the 90% and 70% solutions, and yellow dye added to the 80% solution. Specific gravity of each solution was measured by carefully pipetting 2mL into a pre-weighed centrifuge tube. The weight of the solution was divided by 2mL to get specific gravity in g/L. Each solution was chilled to 4˚C, then 250µL was carefully layered into a 2mL centrifuge tube such that the solutions did not mix. 200µL of biomass was pipetted on the top layer and the tubes were centrifuged at 1000g for 30 minutes at 4˚C.

Results and Discussion

Base Process Design

We began by modeling and conducting a techno-economic analysis (TEA) of the baseline process summarized in Figure 1. We considered processing 20,800 tonnes/yr of manure at a 1,000 animal unit dairy farm using existing technology (Supp Fig 1). This wastewater stream contains 12.7 tonnes/yr of P and 76.4 tonnes/yr of N, though this content can be highly variable by farm and by season. Initial measurements determined that the cyanobacteria strain PCC 7002 has a phosphorus density of 0.017g P per g biomass, which determines its P-recovery capacity. From this we calculated that processing the available P load in the digestate input stream would require the production of 522 tonnes/yr of cyanobacteria biomass. This product is not only significantly more nutrient-dense than raw manure, but also has a significantly lower N:P ratio of 2.4:1, thus facilitating nutrient balancing. The process was assumed to have a lifetime of 15 years during which it operates 365 days per year at an average daylight intensity of 350 µmol/m^2/s, and we assumed that biomass is harvested every 3 days. Approximately 644 tonnes/yr of methane are produced from AD, of which 71% is assumed to be exported off-site while the remainder is combusted to generate

821 MWh/yr of on-site electricity. The combustion of methane enables the utilization of generated CO_2 to run the cyanobacteria bioreactors, eliminating the need to supply additional CO_2. Annualized capital costs were calculated based on a 15% discounted return on investment (DROI) (a typical standard industry benchmark) and a process lifetime of 15 years, with monetary values assigned in terms of USD from the year 2020. The baseline process model and TEA is used as a comparative framework for analyzing how improvements of different aspects of the process impact overall costs and resource use.

Cultivation systems (bioreactors) used in large-scale cyanobacteria growth operations can be quite sophisticated and expensive. Given that this process is designed to be a low-intensity and small-scale operation, we explored different avenues for developing lower cost setups. Using published price information from distributors, we determined that a plastic bag photobioreactor (b-PBR)[15] assembly that uses ground solar panel racks as the mounting hardware significantly reduces the total capital investment (TCI) of the reactors. From this analysis we estimated the capital cost for the b-PBRs to be 0.213 MMUSD, while the cost of the remaining equipment, obtained from values reported in the literature, was 3.682 MMUSD. This resulted in a TCI of 3.895 MMUSD and a total operating cost (TOC) of 0.837 MMUSD/yr. A detailed breakdown of the TCI and TOC across the various sections/components of the process can be found in Supplementary Figure 2.

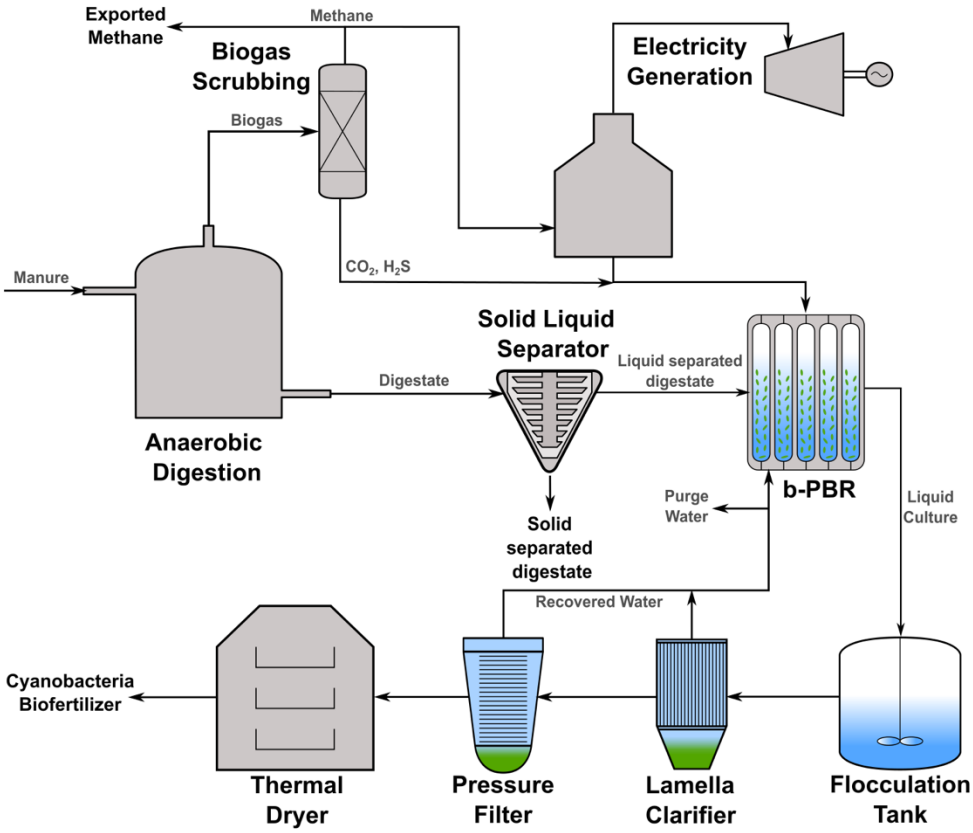

Figure 1. Schematic representation of proposed baseline nutrient recovery process from manure. The anaerobic digestion system produces biogas, which is separated into a pure methane stream and a mixed CO2/H2S stream. A fraction of the methane is exported while the rest is used to generate electricity and carbon dioxide. Liquid digestate from the anaerobic digestion system passes through a solid liquid separator, removing suspended solids. The liquid digestate fraction is combined with CO_2 generated from combustion to cultivate cyanobacteria biomass in a bag photobioreactor (b-PBR). Cyanobacteria culture is concentrated via flocculation, clarification, and filtration, while

recovered water is recycled with 5% purged to prevent contaminant buildup. Concentrated biomass is fully dried to generate a nutrient rich biofertilizer.

Using the calculated TCI and TOC values, we estimated that the process had a total annualized cost (TAC) of 1.689 MMUSD/yr. The cyanobacteria biomass was assigned a value of $0.03/kg, based on the cost of obtaining the equivalent amount of nutrients from diammonium phosphate (DAP); the exported CH_4 and generated electricity were priced at market value. The sale of these three products generated 0.234 MMUSD/yr of revenue, which is enough to cover 14% of the TAC. The remaining revenue was obtained by assuming the process operates as a service provider and charges a fee, on a USD per kg of P recovered basis, for recovering the nutrients in manure (analogous to a wastewater treatment plant). We calculated the phosphorus recovery charge (PRC) to be 117 USD/kg P in our base case model. For comparison, previous work has shown that P runoff has a socioeconomic cost of approximately 75 USD/kg P.[7] This indicates that recovering the P in manure using the baseline process is 57% more expensive than the cost of current manure management practices. This gap in process value highlights the need for further process optimization.

From a resource use perspective, we determined that the baseline process requires 24,172 m^3/yr of water and 2,549 MWh/yr of energy. This is roughly equivalent to the amount of water consumed by 389 dairy cows and the energy needed to care for 2,549 dairy cows. Given that the case study considers a herd size of 1000 cows, this would represent a significant increase in resource use per head. Additionally, the b-PBRs would require a land area of 23.4 acres; for comparison, a 6-foot lagoon that can hold six months-worth of the manure fed to the process (recommended storage size) requires only 1.5 acres of land. The large footprint of the baseline process combined with the high resource use would make adoption by farmers unlikely, again highlighting the need for process optimization.

Our TEA analysis also revealed that the cyanobacteria cultivation and recovery sections (back-end section) account for 54% of the TCI, 66% of the TOC, 86% of the energy use, and 100% of the water consumption (see Supp Fig 2). Therefore, developing solutions that reduce the size of these systems can significantly reduce resource consumption and improve the process performance metrics. To identify the key variables in the back-end section, we performed sensitivity analysis by varying four of our process variables by ±25% and observing the changes in several process metrics (Figure 2). Batch time was the least significant variable to optimize (Figure 2a), likely due to the assumed 3-day batch time causing a 25% swing to be miniscule. We investigated cyanobacteria biomass yield, as we assumed that optimizing photon flux to biomass would improve efficiency; however, the economic metrics do not support this (Figure 2b). The design of the b-PBR seemed like a promising direction, with the surface area to volume ratio (SA:V) improving resource use by 7-40% (Figure 2c). However, economic metrics were less impacted by SA:V, with a less than 10% change in PRC and TAC. The most promising variable identified was P density, which describes the amount of P absorbed per kg of biomass (Figure 2d). Specifically, we found that increasing P density by 25% improves economic metrics by 10-11% and resource usage by 20-34%. Across all six process metrics considered, P density had the largest impact of all the modeled variables, motivating us to design a cyanobacteria strain with optimized P density as the most likely path to improving overall process performance.

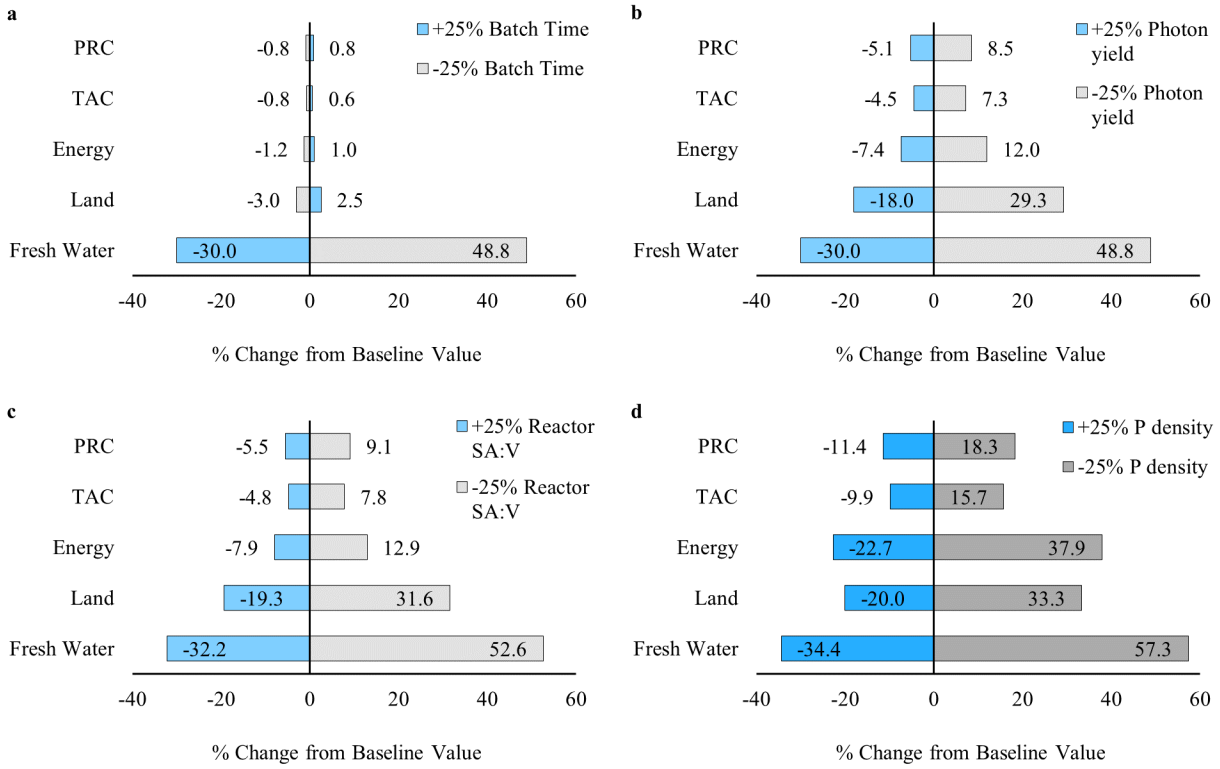

Figure 2. Impacts of modifying process variables by ±25% on performance metrics. Modeled metrics are PRC, TAC, energy use, land use, and water use. Variables investigated are (a) batch time, (b) biomass photon yield, (c) reactor surface area to volume ratio (SA:V), and (d) P density of the cyanobacteria biomass. Darker color signifies the most significant change in each performance metric across the four variables.

Mutant Design

To increase P density in the model cyanobacteria PCC 7002, we chose to focus on maximizing phosphate import, which is under tight genetic control. As shown in Figure 3a, there are two main phosphate transporters in bacteria: the high-affinity low-rate *pstSCAB* system and the low-affinity high-rate *pit* system.[36] Both systems are generally controlled by the *pho* regulon, which manages the global response to phosphate conditions. *pstSCAB* is typically active in low phosphate conditions and *pit* is generally either constitutively active or expressed only in high phosphate conditions. Phosphate uptake is tightly controlled, and our first objectives were to remove native regulation and increase expression of both phosphate transporters.

In 7002, *pstSCAB* is separated into two loci: the *pstSCA* operon and a separate *pstB* gene. We reintroduced a copy of *pstB* (sourced from *Synechococcus elongatus* UTEX 2973 to prevent recombination) as well as a high expression level optimized lac promoter cLac143,[37] generating strain PST+ (Figure 3b). There is no native *pit* homolog in 7002, so we integrated a codon optimized *E. coli pitA* under cLac143 control into a previously characterized neutral site downstream of *glpK*,[38] generating strain PIT+ (Figure 3b). Both mutants are maintained under gentamycin selection, and for accurate comparisons we constructed a control strain with gentamycin resistance marker integrated into the *glpK* neutral site (wild-type).

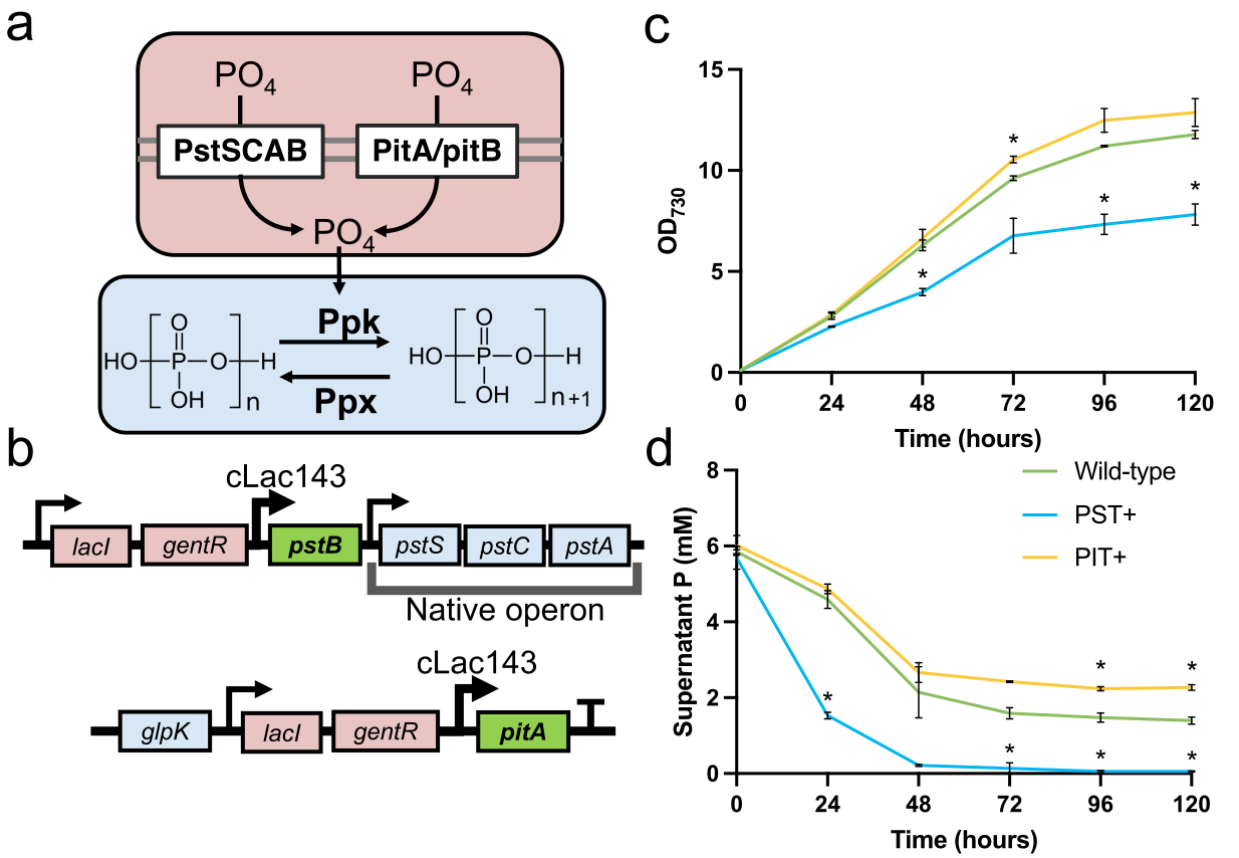

Figure 3. Upregulating phosphate uptake. (a) Diagram of the systems for phosphate import and storage. (b) Genetic constructs for upregulating phosphate import in PCC 7002. Native genes shown in blue, heterologous phosphate uptake genes shown in green, and selection/control genes shown in red. (c,d) wild-type, PST+, and PIT+ grown in 5mM phosphate media, with optical density shown in (c) and residual phosphate in the cell free supernatant shown in (d) in mM. Welch's T-test was used to compare means to wild-type with Bonferroni correction (*$p < 0.05$).

To test initial phosphate uptake rates, all three strains were first propagated in Media A,[30] which has an initial phosphate concentration of 370µM. We observed no change in biomass density between PST+ and wild-type (Supp Fig 3), but, surprisingly, *pitA* overexpression increased final biomass density from 4.2 g/L to 5.5 g/L. Phosphate was depleted in all 3 strains within 48 hours, with a majority of uptake occurring in the first 24 hours. Due to the rapid phosphate uptake, differences between the three strains could not be observed. To look for changes in phosphate uptake rate, initial phosphate concentration was increased to 6mM by addition of KH_2PO_4. In these conditions, *pstSCAB* overexpression significantly reduced biomass density as measured by optical density (Figure 3c). Overexpression of *pitA*, however, increased growth similarly to the 370µM condition, though not significantly. Phosphate depletion occurs faster in *PST*+ over wild-type, with significantly lower residual phosphate levels at 24 hours and complete phosphate depletion within 72 hours (Figure 3d). Overexpression of *pitA* caused an unexpected decrease in phosphate accumulation in these conditions, from ~1.4mM residual P in the control to ~2.3mM in the *pitA* overexpression mutant. These results highlighted *pstSCAB* as the better phosphate transporter in these conditions, and so we chose the strain PST+ for further optimization.

Fed Batch Bioreactor Performance

Next, we set out to find the maximum phosphate storage capacity in our strains by supplying an excess of phosphate. We opted for a fed batch scheme, tuning phosphate delivery rate to roughly match phosphate uptake rate. To accomplish this, we utilized previously described custom photobioreactors[34] with a working volume of 800mL, 750µE/m^2/s illumination, and 5% CO2 sparged at 0.1L/min. Phosphate feeding was capped at ~1.4mL/hour from a peristaltic pump to minimize changes to reactor volume. Several phosphate concentrations were tested before settling on 200mM K_2HPO_4, which delivers ~350mmol/L/hr (Supp Fig 4).

An issue that arose with high concentrations of phosphate in Media A was precipitation of calcium phosphate. In biological phosphorus removal systems, this property is utilized to recover phosphate from wastewater.[39] However, this property makes accurate phosphate quantification difficult when looking for maximal phosphate uptake rate. We found that reducing calcium concentration in the media from 50mM to 10mM was sufficient to make precipitation undetectable (Supp Fig 5). We called this modified formulation Media C, and all subsequent experiments were performed using the modified formulation. In early fed-batch photobioreactor runs we observed an unexpected decrease in biomass after 72 hours of growth, ultimately leading to photobleaching of the culture (Supp Fig 4). To avoid this, we terminated runs at 72 hours of growth and harvested biomass for analysis.

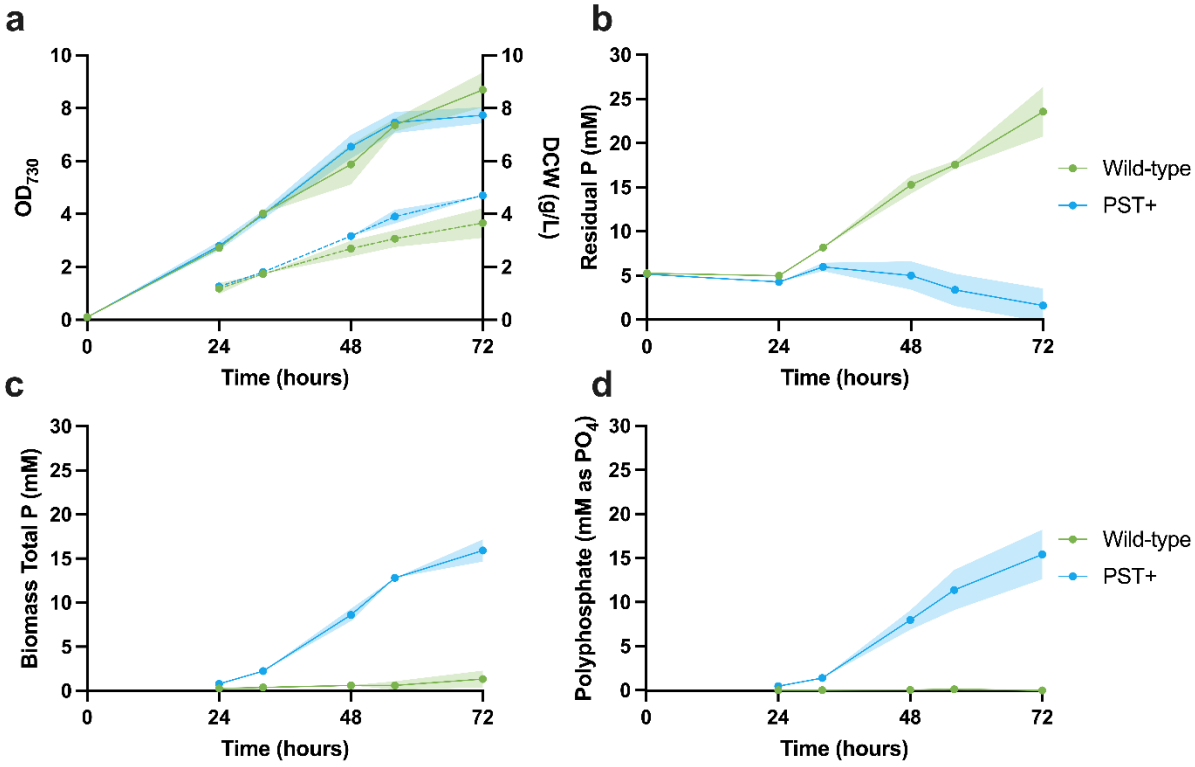

Figure 4. Fed-batch photobioreactor performance. (a) Growth in fed batch photobioreactor measured via optical density (solid lines) and dry cell weight (dotted lines). (b) Free phosphate remaining in the supernatant after centrifugation. (c) Total phosphorus in the biomass fraction as measured by acid persulfate digestion. (d) Polyphosphate concentration measured by enzymatic kit (Aminoverse).

Summarized in Figure 4 are the results of 3 independent fermentation runs each of wild-type and PST+. Growth, shown in Figure 4a, is comparable between strains, with optical density (OD) increasing linearly up to 72 hours. Dry cell weight (DCW) also increases linearly, though we observed a consistent but non-significant trend of higher DCW in PST+, suggesting that the mass per cell may be increased. Residual phosphate in the growth media accumulates rapidly in wild-type, as native regulation shuts off phosphate import in high P conditions (Figure 4b). In PST+, residual phosphate accumulates slightly before being almost fully consumed, which is reflected in the total P in the biomass fraction (Figure 4c). PST+ accumulates significantly more phosphate compared to wild-type, primarily stored in the form of polyphosphate (Figure 4d). Together, these data show that PST+ can be grown to very high P content with an elevated P uptake rate that is uninhibited by extracellular phosphorus concentration.

To evaluate our cyanobacteria biomass as a potential fertilizer, we sent samples for major elemental analysis (Midwest Laboratories), with the results summarized in Table 1. Notably, PST+ significantly increased biomass phosphorus over wildtype by more than 8-fold. Conversely, the N/P ratio decreased from 2.4 to 0.2, which is crucial for biofertilizer as a low N/P ratio allows farmers to apply phosphorus according to plant demands without over-applying nitrogen or vice-versa.

These changes represent a massive shift in the stoichiometry of the biomass. The Redfield ratio describes the typical C:N:P balance of oceanic algal biomass and is typically reported as 106:16:1.[40] Our wildtype culture grown in high phosphorus fed batch shifts this ratio to about 100:10:4, increasing relative phosphorus concentration at the expense of nitrogen. The PST+ strain shifts the ratio even further to roughly 100:13:62, highlighting the scale of elemental rewiring in this strain.

Sample	Carbon (%)	Nitrogen (%)	Phosphorus (%)	Potassium (%)	Magnesium (%)	Calcium (%)	Sulfur (%)	Sodium (%)	Iron (ppm)
Wild-type 1	**44.7**	4.3	**0.9**	**1.1**	0.2	0.1	0.3	1.9	220
Wild-type 2	**35.9**	3.6	**3.3**	**1.1**	3.5	0.1	0.3	1.5	186
Wild-type 3	**42.9**	4.2	**0.9**	**1.5**	0.3	0.1	0.3	2.5	303
PST+ 1	**23.5**	3.2	**14.7**	**7.0**	3.4	0.0	0.2	1.2	138
PST+ 2	**24.0**	3.0	**14.2**	**7.3**	3.3	0.0	0.2	1.3	168
PST+ 3	**22.7**	3.1	**14.3**	**7.0**	3.3	0.0	0.2	1.6	164
Average Wild-type	**41.1 ± 4.6**	4 ± 0.4	**1.7 ± 1.4**	**1.2 ± 0.2**	1.3 ± 1.9	0.1 ± 0	0.3 ± 0	1.9 ± 0.5	236.3 ± 60.2
Average PST+	**23.4 ± 0.7**	3.1 ± 0.1	**14.4 ± 0.2**	**7.1 ± 0.2**	3.4 ± 0.1	0 ± 0	0.2 ± 0	1.4 ± 0.2	156.7 ± 16.3
p value	*	ns	**	****	ns	ns	ns	ns	ns

Table 1. Elemental composition of biomass harvested from fed batch PBRs. Each column represents element content as a w/w percent of total biomass, with iron represented as ppm. Welch's T-test was used to compare means with Bonferroni correction (*$p < 0.05$, **$p < 0.005$, ****$p < 0.00005$)

Increased Settling Velocity of the PST+ strain

While working with the PST+ strain, we observed that high P biomass would settle out of culture much faster than the wild type. Settling velocity is a key variable for biological phosphorus recovery, as it determines the size and throughput of the flocculation tank for dewatering (Figure 1). To observe this phenomenon qualitatively, we performed a 96-well plate based settling assay. As depicted in Figure 5a, cells settling in a dome shaped well create a pellet of high absorbance biomass when observed from below. By monitoring this increase in absorbance over time and normalizing to the absorbance of a fully settled

pellet, changes in settling velocity can be compared between strains. We observed a trend across 36 replicates (wells) of faster settling rate and increased final settled percentage within the first 30 minutes (Figure 5b).

To further explain this phenomenon, we returned to Figure 4a and noted that the cell mass to OD ratio is increased in the *pstSCAB* mutant. We then hypothesized that the density of the individual cells may be increased. A previous study used a $CsCl_2$ density gradient to measure individual cell density of algal biomass,[35] where bands of ice cold $CsCl_2$ at increasing concentrations are carefully layered in a tube to keep density regions distinct. Culture is then layered on top and centrifuged gently, causing the cells to settle at the interface between two density layers. In Figure 5c, each layer is labeled and colored with alternating dyes for visibility. Wild type and PIT+ biomass behaved similarly and settled at the interface between 1.49g/L and 1.56g/L. However, PST+ biomass pelleted fully, meaning the density of the biomass is greater than the highest density measured of 1.73g/L.

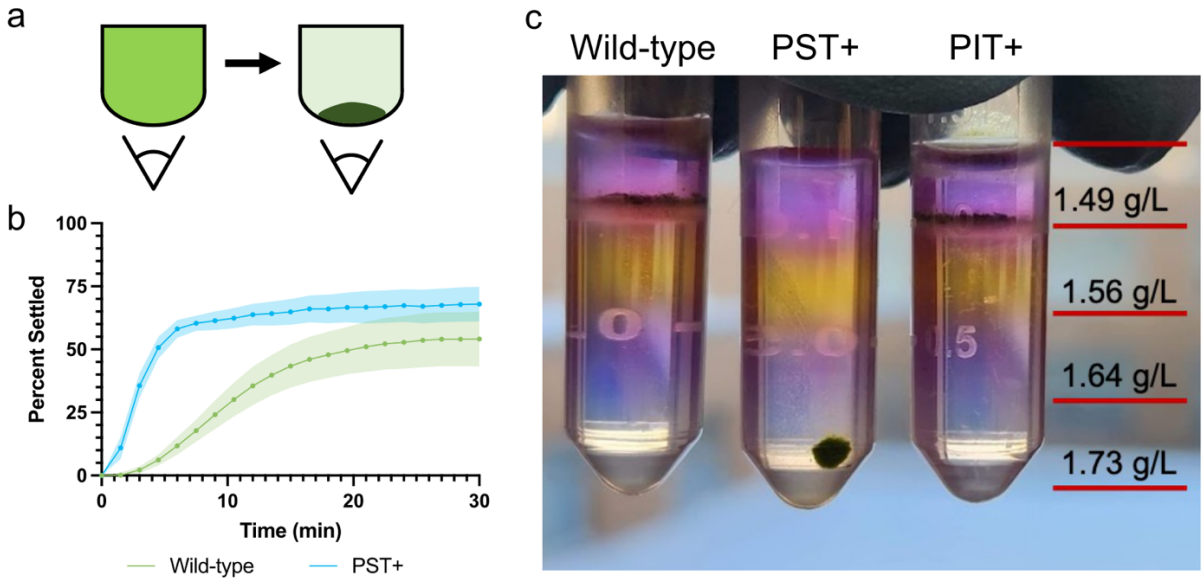

Figure 5. Increased settling rate and biomass density (a) 96-well plate based settling assay. As cells settle to the bottom of the well, absorbance increases as shown in the inset. Settling over time represented as percent of fully settled, where zero is defined as the absorbance at 0 min and 100% is defined as the absorbance of a centrifuged biomass pellet (n=36). (b) Density centrifugation gradient of three strains. Each colored band represents a different density of $CsCl_2$ as noted in the legend.

Settling velocity and density are primarily important variables for the first step of the dewatering train, passive dewatering via lamella clarifier. These are settling tanks with specialized geometry to separate culture into a clean water stream and biomass enriched stream, and their design depends on the settling velocity of the particles in solution. We can estimate particle settling via Stoke's velocity formula, and assuming cell size and culture viscosity are unchanged, the lower limit density values observed correspond to a 49% increase in estimated settling velocity. As lamella clarifiers are assumed to scale linearly in size with settling velocity, this corresponds to a 49% decrease in the size of clarifier required, reducing TCI and

land area of the process. This estimate does not account for flocculation, which can occur naturally and increase settling velocity further, likely making this an underestimate of the true settling velocity and a slightly conservative overestimate of the dewatering cost.

Process Design With PST+ Engineered Strain

Using the phosphorus density values observed in the engineered PST+ strain, we updated our process model and techno-economic analysis to evaluate the impact of our cyanobacteria strain optimization (see Figure 6). Using the PST+ strain improves process performance across all considered metrics when compared to wild-type. The increase in P density resulted in a reduced need for cyanobacteria biomass, which in turn reduced the process throughput and the TAC by 53%, as the back-end (cultivation and recovery) is much smaller when compared to the baseline process. The PRC decreased by 59% to 48 USD/kg P, which is 35% lower than the socioeconomic cost of P runoff (75 USD/kg P).[7] The energy demand decreased by approximately 68%. Makeup water is no longer required, as the manure feed contains enough water to make up for the losses in the product recovery section. Additionally, the land required for the b-PBRs was reduced by 88% (to 3 acres), similar to the footprint required for manure storage on a 1000 cow farm.

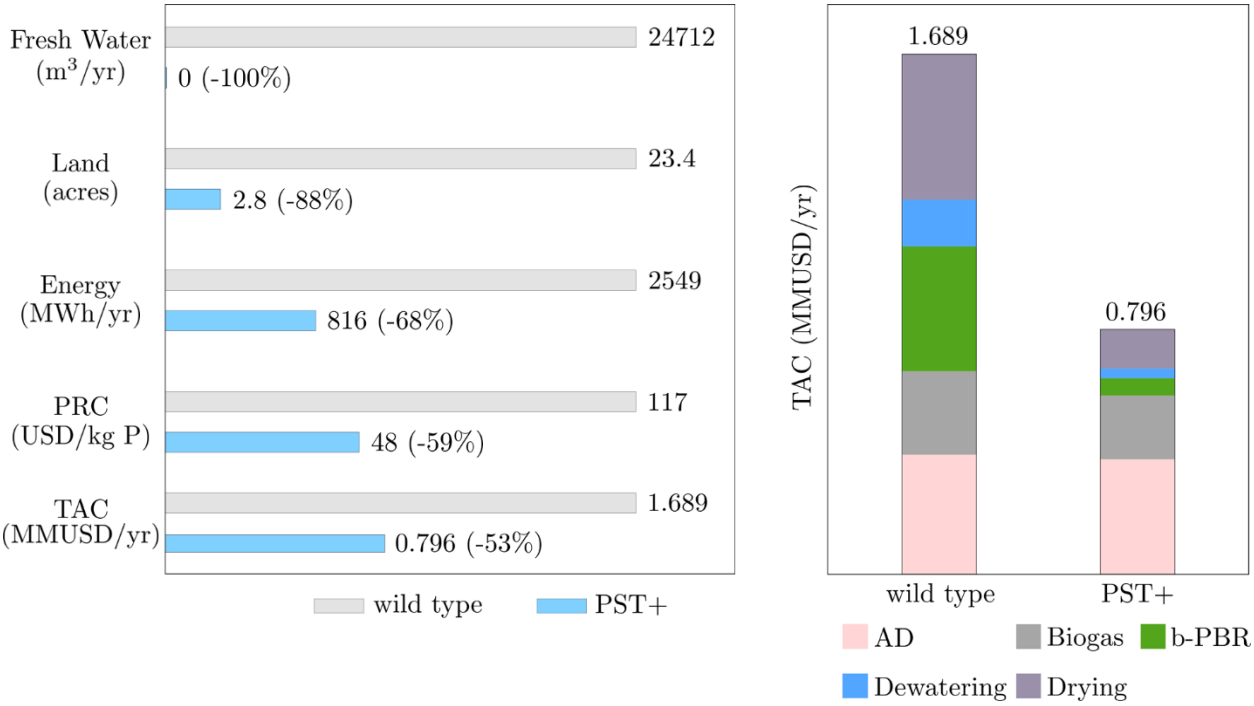

Figure 6. Process metrics using wild-type and the PST+ strain. (a) Resource use and economic metrics. Total value for each strain shown to the right of each bar, with the percentage reduction from the wild-type to the PST+ strain shown in parentheses. (b) Total annual cost (TAC) for process for wild-type and the PST+ strain, broken down by the relative cost of each module as a percentage of the total cost.

Increasing phosphorus density dramatically reduces the amount of cyanobacteria biomass required to capture P by a factor of 8.5. This results in major changes to process design and operation. First, the AD system now produces more than enough CO_2 to meet the carbon needs of the cyanobacteria, making

combustion of the CH_4 for CO_2 generation unnecessary. As a result, all the generated methane can be exported off-site, as is the norm at existing AD facilities. This allows us to reduce the capital cost by removing the electricity generator from the process (shown in Supp Fig 1) and increase the revenue generated from the biogas. Second, the reduction in water demand requires that the percentage of material purged be increased from 5% to 18% to close the material balance. However, this still represents a reduction in the purge flowrate of 57%.

Examining the breakdown of the TAC across the various sections of the process (Figure 6b) shows the extent to which the PST+ strain reduces the size of the cultivation and harvesting sections. While the back-end accounts for 61% of the total cost when the wild-type strain is used, this is more than halved to 27% when using the mutant strain. On a nominal basis, this represents a decrease in the cost of the back-end from 1.030 MMUSD/yr to 0.215 MMUSD/yr, nearly a 5-fold reduction. Given that the PRC accounts for 75% of the total revenue, these results indicate that deploying the back-end as a stand-alone process using the PST+ strain can significantly increase its value. While this configuration results in the loss of the biogas revenue stream, the PRC decreases 51% to 23 USD/kg P due to the 3.7-fold reduction in the TAC when compared to the full process.

Further improvements can be obtained if we consider operating without the thermal dryer, which has a total cost greater than that of the b-PBRs and dewatering train combined. The stream that exits the pressure filter is ~27% biomass by weight. Using the PST+ mutant, this stream has a P density of 0.039 g P/g effluent, 2.3 times greater than the P density of dry wild-type biomass and 64 times greater than that of manure. As a result, completely drying the biomass might not be the most economical option, especially if it will be used locally. The TAC of the back-end without the dryer is 0.093 MMUSD/yr, resulting in a PRC of 9.2 USD/kg P, this is 88% less than the socioeconomic cost of P runoff. Note that this is equivalent to charging 0.015 USD/gal of manure processed, which is comparable to the 0.005 USD/gal of sewage charged by the Madison Metropolitan Sewage District. This result demonstrates that the PST+ strain may enable a scalable nutrient recovery process that operates at a similar price point as an existing urban wastewater treatment facility, thereby delivering a significant socioeconomic benefit.

Conclusions

Cyanobacterial phosphate accumulation can potentially solve two major problems facing modern agriculture: recovery of valuable phosphorus resources and reduction of ecological damage from nutrient mismanagement. In this work, we present a process for the recovery of phosphorus from dairy manure. Due to the relatively high cost of cyanobacteria cultivation, we explored the impact of several design variables on process performance and determined that increasing phosphate density can serve as an effective solution for reducing process cost. We demonstrated experimentally that by deregulating expression of the phosphate transporter operon *pstSCAB* we were able to increase phosphate uptake 8.5-fold and maintain phosphate uptake during stationary phase. Even without modifications to polyphosphate production, this strain showed increased accumulation of polyphosphate over wild type during stationary phase. Techno-economic analysis shows that the new strain reduced process costs by 53%, resulting in a 59% reduction in the levied phosphorus recovery charge. The process also required 68% less energy, 88% less land, and fully eliminated the need for freshwater.

One key simplifying assumption in our model is that rather than modeling diurnal cycling, we have opted instead to assume a constant average light intensity of 350μE/m^2/s. By averaging the sunlight

experienced across a full 24 hours, we are able to account for the reduced growth rate and phosphorus uptake rate during the dark hours. However, future work is needed to expand this model to better account for diurnal cycling, and future experimental work will help better define the metabolism of our cyanobacterial mutant in the dark. These will be key steps to improve the model and identify potential hurdles towards economic viability that can be addressed in future process- and bio-engineering work.

An analysis of the breakdown of the total cost by section revealed that the cost distribution is heavily skewed towards the anaerobic digestion and biogas recovery units when using the mutant cyanobacteria strain. As a result, only 27% of the revenue generated is needed to pay for the cyanobacteria cultivation and dewatering units. From this we determined that deploying the back-end as a stand-alone section is a more economical option for phosphorus recovery, with a tradeoff of reduced methane revenue. This highlights interesting trade-offs that arise from the tight integration of biomass, water, energy, and nutrients in the process. We calculated that if we deploy only the cultivation and dewatering systems the process can operate with phosphorus recovery credit that is an additional 81% lower and is comparable to the sewage treatment fee charged by an urban wastewater treatment plant. Moving forward, we will study the viability of these stand-alone process configurations, especially the effects of transportation costs for digestate and cyanobacteria biomass. We also highlight the need to further analyze the value of cyanobacteria as biofertilizer, application of which can provide additional benefits such as increasing soil carbon and benefiting soil microbiome communities. These directions could further improve economic viability and provide a clearer picture of the parts of the process to further optimize.

Author Contributions

TAC, LDG, BFP, and VZ conceived the study. LDG built the techno-economic model. TAC carried out cyanobacteria engineering and cultivation experiments. BCL assisted with validation modeling. LDG and TAC wrote the paper, and all authors provided feedback on the manuscript.

Conflicts of Interest

There are no conflicts to declare.

Data Availability Statement

All code needed to reproduce the presented computational results can be found at:
https://github.com/zavalab/Photosynthetic-Nutrient-Recovery
To request strains or plasmids described in this work, contact Brian Pfleger at brian.pfleger@wisc.edu

Supporting Information

Supplementary Methods: Technoeconomic Analysis Methodology, Environmental Analysis, &Mass and Energy Balances for Unit Operations.
Supporting Figures and Tables: Detailed model diagram with labeled modules and inputs (Figure S1). Detailed breakdown of TOC and TCI (Figure S2). Growth and phosphate uptake in 0.5mM phosphate media (Figure S3). Fed batch PBR results of TAC60 at different P feed rates (Figure S4). Precipitation of calcium phosphate at varying calcium concentrations (Figure S5). Mass flow of the process with electricity generation for the base case using the wild-type strain (Table S1). Mass flow of the process without electricity generation using the mutant strain (Table S2). Economic variables, Total Capital Investment

(TCI) and Total Operating Cost (TOC) (Table S3). Process design parameters (Table S4). Capital Costs (Table S5). Variable operating costs (Table S6). Product yield factors (Table S7). Mean concentrations of total solids, total nitrogen, total phosphorus and total ammoniacal nitrogen (TAN) for manure in the anaerobic digester and solid liquid separator (Table S8).

Acknowledgements

This work was funded by NSF EFRI DCheM: Distributed Photosynthetic Recovery of Livestock Waste Nutrients for Sustainable Production of Fertilizers, Award #2132036. TAC was supported by an NHGRI training grant to the Genomic Sciences Training Program 5T32HG002760. LDG was supported by the University of Wisconsin Graduate Engineering Research Scholars Fellowship and the PPG Fellowship.

References

1. C. Lu and H. Tian, "Global nitrogen and phosphorus fertilizer use for agriculture production in the past half century: Shifted hot spots and nutrient imbalance," *Earth System Science Data*, vol. 9, no. 1, pp. 181–192, Mar. 2017, doi: 10.5194/ESSD-9-181-2017.
2. D. Cordell, J. O. Drangert, and S. White, "The story of phosphorus: Global food security and food for thought," *Global Environmental Change*, vol. 19, no. 2, pp. 292–305, May 2009, doi: 10.1016/J.GLOENVCHA.2008.10.009.
3. D. L. Childers, J. Corman, M. Edwards, and J. J. Elser, "Sustainability Challenges of Phosphorus and Food: Solutions from Closing the Human Phosphorus Cycle," *BioScience*, vol. 61, no. 2, pp. 117–124, Feb. 2011, doi: 10.1525/BIO.2011.61.2.6.
4. X. Qin *et al.*, "How long-term excessive manure application affects soil phosphorous species and risk of phosphorous loss in fluvo-aquic soil," *Environmental Pollution*, vol. 266, p. 115304, Nov. 2020, doi: 10.1016/J.ENVPOL.2020.115304.
5. K. Reid, K. Schneider, and P. Joosse, "Addressing Imbalances in Phosphorus Accumulation in Canadian Agricultural Soils," *Journal of Environmental Quality*, vol. 48, no. 5, pp. 1156–1166, Sep. 2019, doi: 10.2134/JEQ2019.05.0205.
6. H. A. Aguirre-Villegas, R. A. Larson, and M. A. Sharara, "Anaerobic digestion, solid-liquid separation, and drying of dairy manure: Measuring constituents and modeling emission," *Science of The Total Environment*, vol. 696, p. 134059, Dec. 2019, doi: 10.1016/J.SCITOTENV.2019.134059.
7. W. J. Dougherty, N. K. Fleming, J. W. Cox, and D. J. Chittleborough, "Phosphorus Transfer in Surface Runoff from Intensive Pasture Systems at Various Scales," Journal of Environmental Quality, vol. 33, no. 6, pp. 1973–1988, Nov. 2004, doi: 10.2134/JEQ2004.1973.
8. W. K. Dodds et al., "Eutrophication of U. S. freshwaters: Analysis of potential economic damages," Environmental Science and Technology, vol. 43, no. 1, pp. 12–19, Jan. 2009, doi: 10.1021/ES801217Q.
9. A. M. Sampat, A. Hicks, G. J. Ruiz-Mercado, and V. M. Zavala, "Valuing economic impact reductions of nutrient pollution from livestock waste," *Resources, Conservation and Recycling*, vol. 164, p. 105199, Jan. 2021, doi: 10.1016/J.RESCONREC.2020.105199.
10. A. G. Dorofeev, Y. A. Nikolaev, A. v. Mardanov, and N. v. Pimenov, "Role of Phosphate-Accumulating Bacteria in Biological Phosphorus Removal from Wastewater," *Applied Biochemistry and Microbiology 2020 56:1*, vol. 56, no. 1, pp. 1–14, Mar. 2020, doi: 10.1134/S0003683820010056.
11. S. M. Saia, H. J. Carrick, A. R. Buda, J. M. Regan, and M. Todd Walter, "Critical review of polyphosphate and polyphosphate accumulating organisms for agricultural water quality management," *Environmental Science and Technology*, vol. 55, no. 5, pp. 2722–2742, Mar. 2021, doi: 10.1021/ACS.EST.0C03566.

12. J. E. Roldán-San Antonio and M. Martín, "Optimal Integrated Plant for Biodegradable Polymer Production," ACS Sustainable Chemistry and Engineering, vol. 11, no. 6, pp. 2172–2185, Feb. 2023, doi: 10.1021/ACSSUSCHEMENG.2C05356.
13. B. Hernández and M. Martín, "Optimal Integrated Plant for Production of Biodiesel from Waste," ACS Sustainable Chemistry and Engineering, vol. 5, no. 8, pp. 6756–6767, Aug. 2017, doi: 10.1021/ACSSUSCHEMENG.7B01007.
14. J. Ma, P. Tominac, B. F. Pfleger, and V. M. Zavala, "Infrastructures for Phosphorus Recovery from Livestock Waste Using Cyanobacteria: Transportation, Techno-Economic, and Policy Implications," ACS Sustainable Chemistry and Engineering, vol. 9, no. 34, pp. 11416–11426, Aug. 2021, doi: 10.1021/acssuschemeng.1c03378.
15. J. N. Clippinger and R. E. Davis, "Techno-Economic Analysis for the Production of Algal Biomass via Closed Photobioreactors: Future Cost Potential Evaluated Across a Range of Cultivation System Designs," Sep. 2019, doi: 10.2172/1566806.
16. V. Carrillo, B. Fuentes, G. Gómez, and G. Vidal, "Characterization and recovery of phosphorus from wastewater by combined technologies," Reviews in Environmental Science and Bio/Technology 2020 19:2, vol. 19, no. 2, pp. 389–418, May 2020, doi: 10.1007/S11157-020-09533-1.
17. N. Shen and Y. Zhou, "Enhanced biological phosphorus removal with different carbon sources," Applied Microbiology and Biotechnology, vol. 100, no. 11, pp. 4735–4745, Jun. 2016, doi: 10.1007/S00253-016-7518-4.
18. M. El-Sheekh, M. M. El-Dalatony, N. Thakur, Y. Zheng, and E. S. Salama, "Role of microalgae and cyanobacteria in wastewater treatment: genetic engineering and omics approaches," International Journal of Environmental Science and Technology 2021 19:3, vol. 19, no. 3, pp. 2173–2194, Apr. 2021, doi: 10.1007/S13762-021-03270-W.
19. L. Wang *et al.*, "Anaerobic digested dairy manure as a nutrient supplement for cultivation of oil-rich green microalgae Chlorella sp.," *Bioresource Technology*, vol. 101, no. 8, pp. 2623–2628, Apr. 2010, doi: 10.1016/J.BIORTECH.2009.10.062.
20. T. C. Korosh, A. Dutcher, B. F. Pfleger, and K. D. McMahon, "Inhibition of Cyanobacterial Growth on a Municipal Wastewater Sidestream Is Impacted by Temperature," *mSphere*, vol. 3, no. 1, Feb. 2018, doi: 10.1128/MSPHERE.00538-17.
21. Z. Rupawalla *et al.*, "Algae biofertilisers promote sustainable food production and a circular nutrient economy – An integrated empirical-modelling study," *Science of The Total Environment*, vol. 796, p. 148913, Nov. 2021, doi: 10.1016/J.SCITOTENV.2021.148913.
22. W. Mulbry, E. K. Westhead, C. Pizarro, and L. Sikora, "Recycling of manure nutrients: use of algal biomass from dairy manure treatment as a slow release fertilizer," *Bioresource Technology*, vol. 96, no. 4, pp. 451–458, Mar. 2005, doi: 10.1016/J.BIORTECH.2004.05.026.
23. J. Coppens *et al.*, "The use of microalgae as a high-value organic slow-release fertilizer results in tomatoes with increased carotenoid and sugar levels," *Journal of Applied Phycology*, vol. 28, no. 4, pp. 2367–2377, Aug. 2016, doi: 10.1007/S10811-015-0775-2.
24. E. Yilmaz and M. Sönmez, "The role of organic/bio–fertilizer amendment on aggregate stability and organic carbon content in different aggregate scales," *Soil and Tillage Research*, vol. 168, pp. 118–124, May 2017, doi: 10.1016/J.STILL.2017.01.003.
25. L. Falchini, E. Sparvoli, and L. Tomaselli, "Effect of Nostoc (Cyanobacteria) inoculation on the structure and stability of clay soils," *Biology and Fertility of Soils*, vol. 23, no. 3, pp. 346–352, 1996, doi: 10.1007/BF00335965.
26. H. M. Goemann *et al.*, "Aboveground and belowground responses to cyanobacterial biofertilizer supplement in a semi-arid, perennial bioenergy cropping system," *GCB Bioenergy*, vol. 13, no. 12, pp. 1908–1923, Dec. 2021, doi: 10.1111/GCBB.12892.

27. C. Ledda, A. Schievano, B. Scaglia, M. Rossoni, F. G. Acién Fernández, and F. Adani, "Integration of microalgae production with anaerobic digestion of dairy cattle manure: an overall mass and energy balance of the process," Journal of Cleaner Production, vol. 112, pp. 103–112, Jan. 2016, doi: 10.1016/J.JCLEPRO.2015.07.151.
28. Y. Pouliot, G. Buelna, C. Racine, and J. de la Noüe, "Culture of cyanobacteria for tertiary wastewater treatment and biomass production," Biological Wastes, vol. 29, no. 2, pp. 81–91, Jan. 1989, doi: 10.1016/0269-7483(89)90089-X.
29. P. Bohutskyi and E. Bouwer, "Biogas production from algae and cyanobacteria through anaerobic digestion: A review, analysis, and research needs," Advanced Biofuels and Bioproducts, vol. 9781461433484, pp. 873–975, Jan. 2012, doi: 10.1007/978-1-4614-3348-4_36.
30. M. Martín and I. E. Grossmann, "Optimal engineered algae composition for the integrated simultaneous production of bioethanol and biodiesel," AIChE Journal, vol. 59, no. 8, pp. 2872–2883, Aug. 2013, doi: 10.1002/AIC.14071.
31. M. Martín and I. E. Grossmann, "Optimal integration of a self sustained algae based facility with solar and/or wind energy," Journal of Cleaner Production, vol. 145, pp. 336–347, Mar. 2017, doi: 10.1016/J.JCLEPRO.2017.01.051.
32. Clark, R. L., McGinley, L. L., Purdy, H. M., Korosh, T. C., Reed, J. L., Root, T. W., & Pfleger, B. F. (2018). Light-optimized growth of cyanobacterial cultures: Growth phases and productivity of biomass and secreted molecules in light-limited batch growth. Metabolic Engineering, 47, 230–242. https://doi.org/10.1016/J.YMBEN.2018.03.017
33. S. E. Stevens, C. O. P. Patterson, and J. Myers, "THE PRODUCTION OF HYDROGEN PEROXIDE BY BLUE-GREEN ALGAE: A SURVEY," *Journal of Phycology*, vol. 9, no. 4, pp. 427–430, 1973, doi: 10.1111/J.1529-8817.1973.TB04116.X.
34. R. L. Clark, L. L. McGinley, D. F. Quevedo, T. W. Root, and B. F. Pfleger, "Construction and Operation of an Affordable Laboratory Photobioreactor System for Simultaneous Cultivation of up to 12 Independent 1 L Cyanobacterial Cultures," *bioRxiv*, vol. 1, p. 153023, Jun. 2017, doi: 10.1101/153023.
35. Eroglu, E. & Melis, A. "Density equilibrium" method for the quantitative and rapid in situ determination of lipid, hydrocarbon, or biopolymer content in microorganisms. *Biotechnology and Bioengineering* **102**, 1406–1415 (2009).
36. H. ROSENBERG, "Phosphate Transport in Prokaryotes," *Ion Transport in Prokaryotes*, pp. 205–248, Jan. 1987, doi: 10.1016/B978-0-12-596935-2.50009-8.
37. A. L. Markley, M. B. Begemann, R. E. Clarke, G. C. Gordon, and B. F. Pfleger, "Synthetic Biology Toolbox for Controlling Gene Expression in the Cyanobacterium Synechococcus sp. strain PCC 7002," *ACS Synthetic Biology*, vol. 4, no. 5, pp. 595–603, May 2015, doi: 10.1021/SB500260K.
38. M. B. Begemann, E. K. Zess, E. M. Walters, E. F. Schmitt, A. L. Markley, and B. F. Pfleger, "An Organic Acid Based Counter Selection System for Cyanobacteria," *PLOS ONE*, vol. 8, no. 10, p. e76594, Oct. 2013, doi: 10.1371/JOURNAL.PONE.0076594.
39. R. Taddeo, M. Honkanen, K. Kolppo, and R. Lepistö, "Nutrient management via struvite precipitation and recovery from various agroindustrial wastewaters: Process feasibility and struvite quality," *Journal of Environmental Management*, vol. 212, pp. 433–439, Apr. 2018, doi: 10.1016/J.JENVMAN.2018.02.027.
40. A.C. Redfield, B. H. Ketchum, and F. A. Richards, "The influence of organisms on the composition of sea water," *The Sea*, vol. 2, pp. 26-77, 1963.

Graphical Abstract

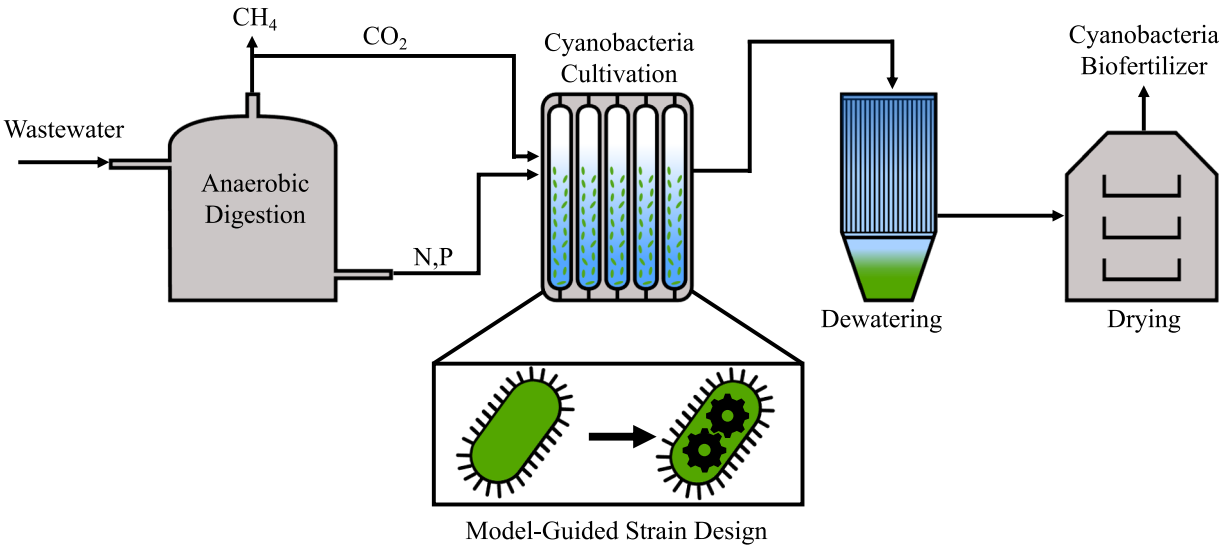

Synopsis

This work describes the design and optimization of a biological treatment for dairy wastewater to reduce phosphorus pollution and circularize the agriculture bioeconomy.